Modification of polypropylene mesh by titanium compound: An *in Vivo* and *in Vitro* study

Yelei Xiao, Xinyue He, Guang Yang, Huanhuan Li, Yu Zhao and Xuehu Wang*

The First Affiliated Hospital of Chongqing Medical University, Chongqing Medical University, Chongqing, China

Objective: Previous basic studies on the use of titanized polypropylene meshes in abdominal external hernia repair are not only limited, but also highly controversial. This study aims to investigate the modification effect of titanium compounds on polypropylene materials and compare the performance of two kinds of meshes both *in vivo* and *in vitro*.

Methods: Human peritoneal mesothelial cells (HMrSV5), human epidermal fibroblasts (HSF), and human monocytic cells (THP-1) were cultured *in vitro* to simulate the abdominal external hernia environment. Titanized polypropylene meshes (Ti) and polypropylene mesh (Non-Ti) were co-cultured with the cells respectively. The effects of titanium compounds on cell growth were determined by cell activity and apoptosis, and the growth of cells on the mesh surface was assessed using a scanning electron microscope and a confocal microscope. *In vivo* experiments, different sizes titanized polypropylene meshes and polypropylene meshes were placed between the external oblique abdominal muscle and the internal oblique abdominal muscle, the parietal peritoneum, the serous layer of the descending colon, and the underside of the femoral nerve in rabbits. The effects of titanium compounds were evaluated by observing the anti-adhesion, anti-contraction, anti-fibrotic properties, and effects on nerves of the mesh.

Results: Titanium compounds effectively reduced the effects of polypropylene material on cell growth, and improved the fixation and adhesion of HMrSV5, HSF and THP-1 (M0) on the surface of titanized polypropylene meshes. Furthermore, titanium compounds improved the adhesion, contraction and fibrosis of polypropylene material, as well as reduced nerve damage. This improvement demonstrated a regular trend with the type of titanized polypropylene meshes.

Conclusion: The titanium compounds improved the biocompatibility of the polypropylene material, which was conducive to the fixation and adhesion of cells on the surface of the meshes, and alleviated the adhesion and contraction of the meshes, and the degree of tissue fibrosis, as well as the influence on nerves.

KEYWORDS

titanium compound, titanized polypropylene mesh, polypropylene mesh, hernia, biocompatibility

1 Introduction

Hernia is a common surgical abdominal condition caused by congenital or acquired defects in the abdominal wall. Depending on the formation of the defect, internal organs such as the omentum and intestines can pass through the defect in the abdominal wall reach to the outside of the abdominal cavity. In the 1980s, tension-free hernia repair appeared, which placed a mesh on the abdominal wall defect for the first time, reinforcing the firmness of traditional surgery. Subsequently, the repair of abdominal wall tissue defects with mesh became a routine surgical method in hernia repair, as it significantly reduces the recurrence rate (Frey et al., 2007). The use of mesh in hernia repair has even become a standard surgical procedure in various countries (Frey et al., 2007; Bland, 2008; Baylon et al., 2017; Elango et al., 2017; Ross et al., 2019; Russo Serafini et al., 2021). At present, polypropylene is the preferred material for abdominal external hernia repair, but its biggest disadvantage is organ adhesion (Leber et al., 1998; Halm et al., 2007; Aydemir Sezer et al., 2017; Hu et al., 2018; Aydemir Sezer et al., 2019). In order to achieve improved biocompatibility, many technologies have combined polypropylene with other materials, such as titanium compounds. Due to titanium compound's inertness, excellent biocompatibility and hydrophilicity, polypropylene materials have been better modified and widely used in clinical practice.

At present, there is still a lack of basic research on titanized polypropylene meshes, and it is not conclusive whether titanium compounds can improve the performance of polypropylene meshes. Many studies have compared titanized polypropylene meshes with a variety of partially absorbable or biological meshes, and it is believed that titanized polypropylene meshes have no obvious advantages in biocompatibility with regard to in inflammation, fibrosis and cell reactions (Junge et al., 2004; Burger et al., 2006; Celik et al., 2009; Pereira-Lucena et al., 2010; Filipović-Čugura et al., 2020). However, many studies have come to different conclusions and believe that the use of titanized polypropylene mesh leads to a reduced level of inflammation, which may be the reason for the reduction of some extracellular matrix components (Scheidbach et al., 2003; Schreinemacher et al., 2009). When it comes to the anti-adhesion properties of a hernia repair mesh, several studies have confirmed the advantages of titanized polypropylene mesh as an inorganic mesh, which may be related to the lower inflammatory reaction caused by the titanized polypropylene mesh (D'Amore et al., 2017; Schug-Pass et al., 2006). However, more studies have come to the opposite conclusion that the absorbable part of other meshes is an important factor in for reducing adhesion (Burger et al., 2006; Schreinemacher et al., 2009). Even when a titanized polypropylene mesh is compared with a pure polypropylene mesh, there are no consistent conclusions in terms of anti-adhesion or anti-shrinkage performance (Schreinemacher et al., 2009; Bouliaris et al., 2019). Moreover, its mechanism and principles have not been described. Previously, a German clinical study confirmed that postoperative complications, especially chronic postoperative pain, could be improved by reducing the material load of titanized polypropylene mesh (titanium loading and polypropylene skeleton), but the mechanism and nerve damage caused by the mesh was not stated (Schopf et al., 2011). In one of our clinical trials, similar clinical results were found: the titanized

polypropylene mesh reduced the occurrence of postoperative foreign body sensation and chronic pain in patients within 1 year after TAPP, especially during physical activities. Compared with ordinary polypropylene mesh, titanized polypropylene mesh can significantly improve the quality of life among patients in some aspects.

Therefore, we conducted this *in vitro* and *in vivo* experiment in order to explore whether the addition of titanium compounds can optimize the performance of pure polypropylene material and whether the type of titanated polypropylene mesh will affect the results.

2 Materials and methods

2.1 Meshes

In order to investigate the effects of titanium compounds on polypropylene materials, two types of meshes with nearly identical physical parameters were used as the main objects of study: Optilene LP® (B. Braun, Spain) and lightweight TiMesh® (PFM Medical, Köln, Germany). The former is a pure polypropylene mesh (denoted as Non-Ti hereafter), and the latter is a polypropylene mesh that contains titanium coating (denoted as Ti hereafter).

To further investigate the performance of different types of titanized polypropylene mesh, we included all three types used in clinical abdominal hernia repair: extralight-weight TiMesh® (16 g/m^2) (Light-Ti), lightweight TiMesh® (35 g/m^2) and heavyweight TiMesh® (65 g/m^2) (Weight-Ti). All the meshes were finely segmented into different sizes according to the experimental requirements, sterilized with ethylene oxide, and then co-cultured with cells or implanted in the experimental body. The parameters of the meshes are shown in Supplementary Table S1.

2.2 *In vitro* study

2.2.1 Preparation and culture of cell lines

In order to study the effects of the mesh on subcutaneous connective tissue, Human Epidermal Fibroblasts (HSF) were used. These were purchased from iCell Bioscience Inc. (Shanghai, China) (Wu et al., 2019) and cultured in DMEM medium supplemented with 10% FBS (PAN, Germany) and 1% penicillin–streptomycin solution (Beyotime, China) under standard cell culture conditions.

In order to investigate the effects of the mesh on the peritoneum, Human Peritoneal Mesothelial cells (HMrSV5) were selected. These cells were derived from the First Affiliated Hospital of Sun Yat-sen University, Guangzhou, China, and were originally established and documented by Roncoet al. (Kajiyama et al., 2007; Shin et al., 2015). Under standard cell culture conditions, the cells were cultured in RPMI 1640 medium supplemented with 10% FBS (PAN, Germany) and 1% penicillin–streptomycin solution (Beyotime, China).

In order to explore the level of inflammation in the environment around the mesh, Human Monocytic Cell lines (THP-1) were utilized. These have been used extensively as a substitute for primary monocytes obtained directly from blood. A prior study supports that the secretory activity of the primary peripheral bold

monocyte is generally well represented by THP-1s (Chamberlain et al., 2009), which can be transformed into M0 macrophages (Sigma, United States) under the induction of PMA (Gordon, 2007; Mosser and Edwards, 2008; Daigneault et al., 2010). The THP-1 were derived from the Hematology Department at the First Affiliated Hospital of Chongqing Medical University, Chongqing, China, and were cultured in RPMI 1640 medium supplemented with 12% FBS (PAN, Germany) and 1% penicillin–streptomycin solution (Beyotime, China) under standard cell culture conditions. Cell cultures were centrifuged with subsequent resuspension in a fresh medium. After evaluating the experimental conditions, the cells density was adjusted to 100,000 cells/cm², and 100 ng/mL PMA (3 d) was added to induce the transformation of THP-1 into macrophages (M0).

2.2.2 Cell proliferation

Cell Counting Kit-8 (CCK-8) (Beyotime, China) was used to measure cell proliferation. Briefly, the cells were separately seeded on the surface of the meshes (1 cm × 1 cm) with a density of 100,000 cells/cm², and were cultured in medium (THP-1 cells need 100 ng/mL of PMA) for 24 h and 48 h. After treatment, 20 μL of CCK-8 solution was added to each well, and the 24-well plate was continuously incubated a 37°C for 1.5 h. Then, the supernatant was collected and transferred to a 96-well plate. The OD value for each well was read at a wavelength of 450 nm to determine the cell viability on a microplate reader (SkanIt Software 2.2). The assay was repeated three times.

2.2.3 Western blotting analysis

Western blotting (WB) analysis was used to measure cell apoptosis. Briefly, the cells were separately seeded on the surface of meshes (1 cm × 1 cm) with a density of 100,000 cells/cm², and were cultured in medium (THP-1 cells need 100 ng/mL of PMA) for 48 h. Total protein was extracted from the cells of each treatment group, using phenyl methanesulfonyl fluoride and RIPA lysis buffer (Beyotime, China), and protein levels were measured using a BCA protein assay kit (Beyotime, China). The proteins were separated by 10% SDS-PAGE and transferred to PVDF membranes (EMD Millipore), and blocked with QuickBlock Blocking Buffer (Beyotime, China) for 30 min at room temperature. Subsequently, the membranes were incubated with primary antibodies overnight at 4°C. Following that, the membrane was washed three times with TBST before being treated with anti-rabbit IgG secondary antibodies for 1 h at room temperature. The membrane was then washed three times with TBST. Protein bands were visible using enhanced ECL chemiluminescence (Cell Signaling Technology, United States). The primary antibodies used were Bax (CST, Beverly, United States), Bcl-2 (CST, Beverly, United States), Cleaved caspases-3 (CST, Beverly, United States), and β-actin (CST, Beverly, United States). Expression levels were normalized to β-actin. The assay was repeated three times.

2.2.4 Scanning electron microscope (SEM)

According to the above method, the meshes were co-cultured with cells for 48 h and fixed in glutaraldehyde. After dehydration and gold spraying, the adhesion of cells on different mesh surfaces was observed by scanning electron microscope (TM4000Plus, Hitachi, Japan). The test was repeated three times.

2.2.5 Confocal microscope

After being cultured for 48 h, the cells cultured on each of the four substrates were first washed in PBS and then fixed for 30 min in 4% formaldehyde. After permeabilization with 0.5% Triton X-100 in PBS for 10 min, Rhodamine–phalloidin (red fluorescence, 1 h, 1:150; Thermo Fisher Scientific) and DAPI (10mim; Thermo Fisher Scientific) were used to fluorescently label the actin and nuclei respectively. Between each step, the samples were washed three times in PBS for 5 min. The antifade polyvinylpyrrolidone mounting mediumv (Beyotime, China) was used to keep the specimens moist, and they were immediately observed and counted under a confocal microscope (Z-axis, Andor, UK).

2.3 In vivo study

2.3.1 Experimental protocol

All experimental animals were obtained from the Laboratory Animal Center of Chongqing Medical University [license number: SCXK (Chongqing) 2012-0001]. Male New Zealand white rabbits (2.0–2.5 kg, 6 ± 1 month old) were used for the experiment. All experimental animals were kept under standard conditions (humidity 45% ± 5%, temperature 23°C ± 5°C, light time 12 h/d) and fed in a single cage. The animal experimental protocol was approved by the Medical Research Ethics Committee of Chongqing Medical University (approval number: 2022-K302, date: 20 June 2022). All experiments were performed in accordance with the Laboratory Animal Care and Use Guide issued by the Ministry of Science and Technology.

2.3.2 Special preparation of mesh

The mesh to be placed in the abdominal wall and intermuscular area was carefully cut to 3 cm × 3 cm before the operation and marked with non-absorbable blue 4-0 prolene sutures (Ethicon, US) at its four corners, and photos were taken to record the preoperative area. The mesh to be placed under the femoral nerve and on the intestinal wall was be cut into approximately 1 cm × 1 cm before the operation. All meshes were sterilized with epoxy hexane and used within the validity period.

2.3.3 Surgical procedures

Different size meshes were placed between the external oblique abdominal muscle and the internal oblique abdominal muscle (Group M), in the parietal peritoneum (Group p), on the serous layer of the descending colon (Group C), and on the underside of the femoral nerve (Group N) in rabbits. The rabbits were divided into these four groups according to different meshes positions (Each group consisted of 72 rabbits). At the same time, three observation points were set up in the experiment, and each group of rabbits were divided into a 7 d group (n = 24), a 30 d group (n = 24), and a 90 d group (n = 24). One of the four kinds of meshes was randomly implanted in each group, with 6 rabbits each.

After anesthesia with 3% pentobarbital solution through the ear border vein, the rabbits were placed on the operating table in a supine position. Skin washing was performed, and hair from the surgical area was removed and disinfected with 10% povidone iodine. Group M: A median incision was done to cut the skin for about 10 cm, and a mesh was placed between the external oblique abdominal muscle and the internal oblique abdominal muscle of the rabbit. Group p: The mesh was placed in the parietal peritoneum of the rabbits and fixed with non-absorbable 5-0 prolene sutures

TABLE 1 The surgical membrane study group score.

Adhesion characteristics	Score
Extent of site involvement	
None	0
<25%	1
<50%	2
<75%	3
<100%	4
Type	
None	0
Filmy, transparent, avascular	1
Opaque, translucent, avascular	2
Opaque, capillaries present	3
Opaque, large vessels present	4
Tenacity	
None	0
Adhesion falls apart	1
Adhesion lyses with traction	2
Adhesion requires sharp dissection	3
Possible total	

(Ethicon, US). Group C: The descending colon was located, the distribution of blood vessels was avoided, and the mesh was fixed on the colon wall (serosa layer) with non-absorbable 5-0 prolene sutures (Ethicon, US). Group N: A 1.5 cm incision was made in the groin area, and after the femoral nerve was fully freed, the mesh was fixed under the femoral nerve. After placement, the incision was closed, sterilized with 10% povidone and covered with sterile excipients. For their recovery, rabbits were returned to their cages to get food and water freely. The animals were examined every 2 days for local and systemic complications.

2.3.4 Necropsy

When the duration of observation was reached, the animals were killed by deep anesthesia with an overdose of 3% pentobarbital solution through the border ear vein. In Group M or Group *p*, the whole anterior abdominal wall was cut off completely to obtain the mesh and surrounding tissues, and the whole process was photographed and recorded to evaluate the adhesion and shrinkage of the mesh. In Group C, the abdominal cavity was entered and the full-thickness descending colon of the mesh area were cut off to obtain the mesh and surrounding tissues. The inguinal region was dissected and the meshes of Group N and surrounding tissues were obtained. All specimens were labeled and fixed with 4% paraformaldehyde for histological analysis. All specimens were histopathologically analyzed by the same pathologist who was unaware of the specimen grouping.

2.3.5 Evaluation of mesh adhesion

While obtaining the mesh in the abdominal wall, the macroscopic adhesion formed by the mesh on the abdominal wall of each rabbit was evaluated and recorded according to the scale. Here. The Surgical Membrane Study Group score (SMSG score shown in Table 1) was used (Listed, 1992). The score was calculated jointly by two different experimenters, and the final score was determined after consultation.

2.3.6 Calculation of mesh shrinkage

The rabbits were sacrificed, and the meshes placed in the abdominal wall and intermuscular space were removed. The marking points of the meshes were photographed again, and the areas marked by the blue prolene sutures before and after the operation were calculated by Image-Pro Plus version 6.0. The shrinkage area was determined by subtracting the mesh area measured postoperatively from the preoperative area. The shrinkage area was divided by the preoperative area for determining the shrinking rate (%).

2.3.7 Histopathology and immunohistochemistry
2.3.7.1 HE

Preparation of 3 μm paraffin sections, hematoxylin-eosin (HE) staining, and quantitative observation of inflammation and granulation connective tissue were conducted under a light microscope (Carl Zeiss, Germany) The Harrell Scoring scale (Harrell et al., 2007) was used for quantitative evaluation of the different parameters of the tissue inflammatory reaction (Shown in Table 2).

2.3.7.2 Sirius red staining

To identify type I and type III collagen, 3 μm paraffin sections were prepared and collagen production was assessed after staining with Sirius red. Under polarization microscopy, collagen type I appeared as a red-orange shades whereas collagen type III displayed a pale-green color (Junqueir, 1978). The Image-Pro Plus version 6.0 was used to calculate the percentage of collagen type I and III. A semiquantitative histological score was assigned to each of the slides, and the mean score of three different fields was calculated.

2.3.7.3 Immunohistochemistry

For immunohistochemical analysis, rabbit monoclonal antibodies against fibronectin (Servicebio, Cat: GB13091) (1:200) and intercellular adhesion molecule 1 (Servicebio, Cat: GB11106) (1:1,000) were used to stain for assessed degree of intercellular fibrosis. The rabbit monoclonal antibodies against GAP-43 (Servicebio, Cat: GB11095) (1:1,000), Caspase-3 rabbit polyclonal antibody (Servicebio, Cat: GB11095) (1:1,000), and MAP-2 rabbit polyclonal antibody (Servicebio, Cat: GB11095) (1:1,000) were used to stain for assessed regeneration and injury of femoral nerve. The antigen-antibody reaction was detected by the alkaline phosphatase-labeled avidin-biotin procedure. Cell nuclei were counterstained for a few minutes in Carazzi's hematoxylin. Tissue sections were examined under a light microscope (Carl Zeiss, Germany). The Image-Pro Plus version 6.0 was used to calculate the positive rate of each staining in the immunohistochemical images. Each slice was given a semi-quantitative histological score and the average score of three different light microscopy fields was calculated.

2.4 Statistical analyses

Images are processed by Image-Pro Plus version 6.0. The data were expressed as the means ± standard error of the mean, and all the statistical tests were performed using the program GraphPad Prism 8.0 computer package (GraphPad Software, Inc., La Jolla, CA, United States) for Windows.

TABLE 2 The Harrell Scoring scale.

Legend	Score
Cell layers at the margins of the granulomas	
1–4 layers	1
5–9 layers	2
10–30 layers	3
>30 layers	4
Inflammatory reaction in the host tissue	
Non-dense, mature fibrous tissue	1
Immature fibrous tissue with fibroblasts and little collagen	2
Dense granular tissue with fibroblasts and many inflammatory cells	3
Mass of inflammatory cells, with disorganization of the connective tissue	4
Inflammatory response on the prosthesis surface	
Fibroblasts, without macrophages or foreign-body cells	1
Isolated foci of macrophages or foreign body cells	2
One layer of macrophages and foreign body cells	3
Multiple layers of macrophages and foreign body cells	4
Tissue maturation	
Dense mature interstitial tissue, similar to normal connective or adipose tissue	1
Interstitial tissue with blood vessels, fibroblasts and a few macrophages	2
Interstitial tissue with giant inflammatory cells, but with permeating connective tissue	3
Mass of inflammatory cells, without permeating connective tissue	4

FIGURE 1
Effect of titanium compounds on cell growth. **(A)** CCK-8 results of the 3 cells co-cultured with the meshes after 48 h; **(B)** WB results of HSF co-culture with the meshes after 48 h; **(C)** WB results of HMrSV5 co-culture with the meshes after 48 h; **(D)** WB results of activated THP-1 (M0) co-culture with the meshes after 48 h.
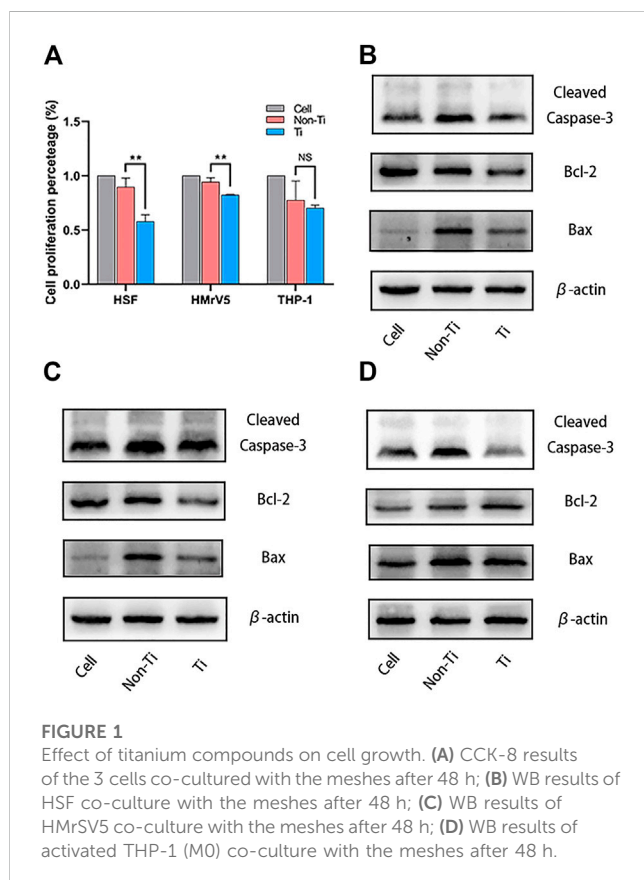
If the data conform to normal distribution and have homogeneity of variance, we will use the method of One-way ANOVA and t-test to compare the differences between different treatment groups. If not, the Mann-Whitney U test was used. $p < 0.05$ was considered significantly different.

3 Results

3.1 Effects of titanium compounds on cell growth

3.1.1 Cell proliferation

After 12 h, there was no significant difference in the proliferation of the 3 cell lines in the two mesh environments. After 48 h, compared with the cell group without treatment, not only did the increment rate of cells in the mesh environment decrease, but the degree and trend of inhibition were also similar. In HSF and HMrSV5 cells, the cell proliferation rate of Non-Ti group was higher than that of Ti group ($p = 0.0021$). However, there was no significant difference in activated THP-1 (M0) (Figure 1A).

3.1.2 Western blotting analysis

Western blotting analysis was used to detect apoptosis-related factors in cells in the two mesh environments. Both the Non-Ti group and the Ti group were observed to have an increase in cell apoptosis, and the quantitative detection of Bcl-2/Bax ratio found that the degree of apoptosis was higher in the Non-Ti group. This difference in the
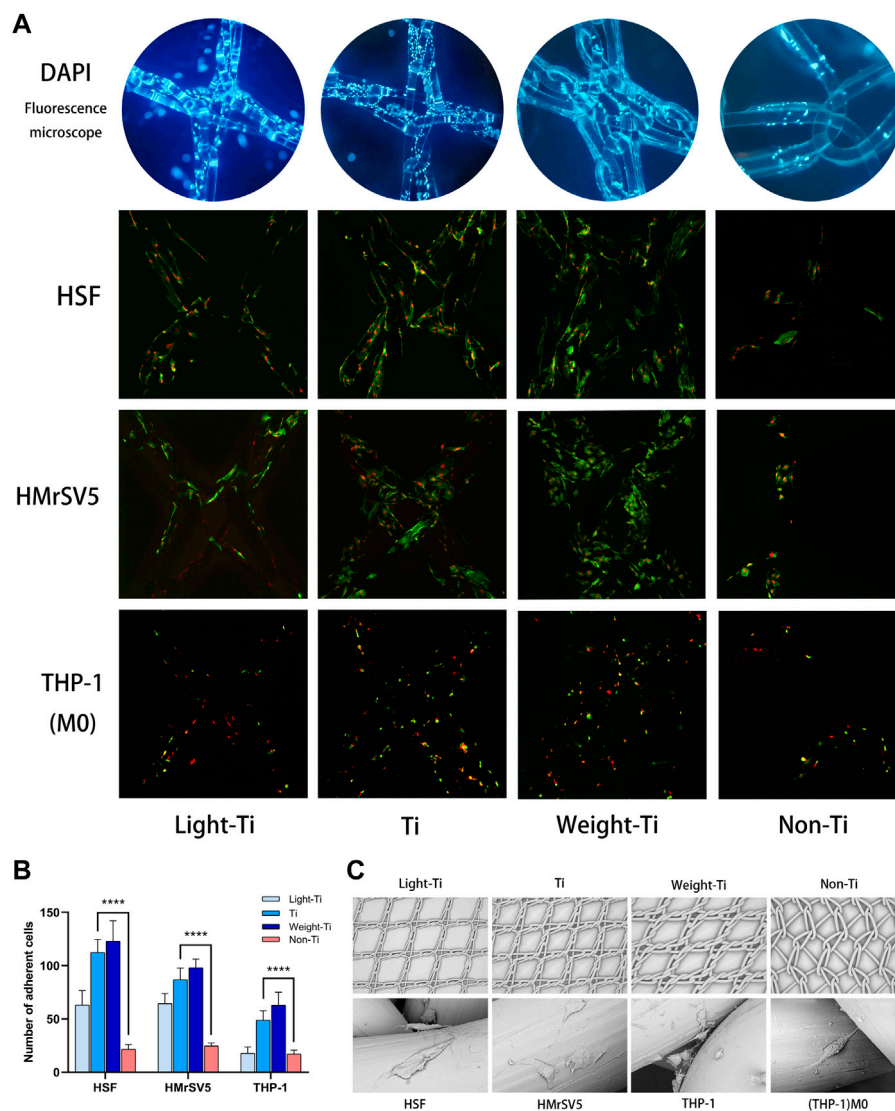
FIGURE 2
Cells growth on the mesh. **(A)** Cells growth on the mesh surface (non-homogeneous cells, not the same culture time) under fluorescence microscopy (DAPI, 1,000x magnification), and cells growth on mesh surfaces (all ×48 h) under confocal microscopy (z-axis imaging, ×1000 magnification); **(B)** statistics of cell adhesion number under confocal microscope (****$p < 0.001$); **(C)** Scanning electron microscopy of the mesh fragments (×20 magnification) and the cell cellular morphology on the mesh (1,000x magnification).

degree of apoptosis was more obvious in HSF and HMrSV5, compared to activated THP-1 (Shown in Figures 1B, C, D respectively).

3.2 Cell growth on the mesh

3.2.1 Confocal microscope

The four meshes were co-cultured with the three kinds of cells. After fluorescent staining, the adhesion and growth of cells in the Light-Ti, Ti and Weight-Ti groups were noted to be significantly superior to the Non-Ti group. The adhesion rates of the three kinds of cells in the Non-Ti group were lower than those in the Ti group ($p < 0.001$), and the cell adhesion rates increased with the rise in Ti-mesh type (Shown in Figures 2A, B).

3.2.2 Scanning electron microscope

Figure 2C shows the gross morphology of the four meshes under the electron microscope, as well as the growth density and morphological characteristics of each cell on the mesh. It is evident that the cell density is consistent with the trend of cell counts after fluorescent immunostaining. Furthermore, as the diameter of the mesh woven monofilament is larger, the morphology of the cells is more complete.

3.3 Necropsy

Figure 3 illustrates the mesh and surrounding tissues when the mesh was placed and collected. In Group M, there is only one case of folding in the Light-Ti group, which is likely related to the placement
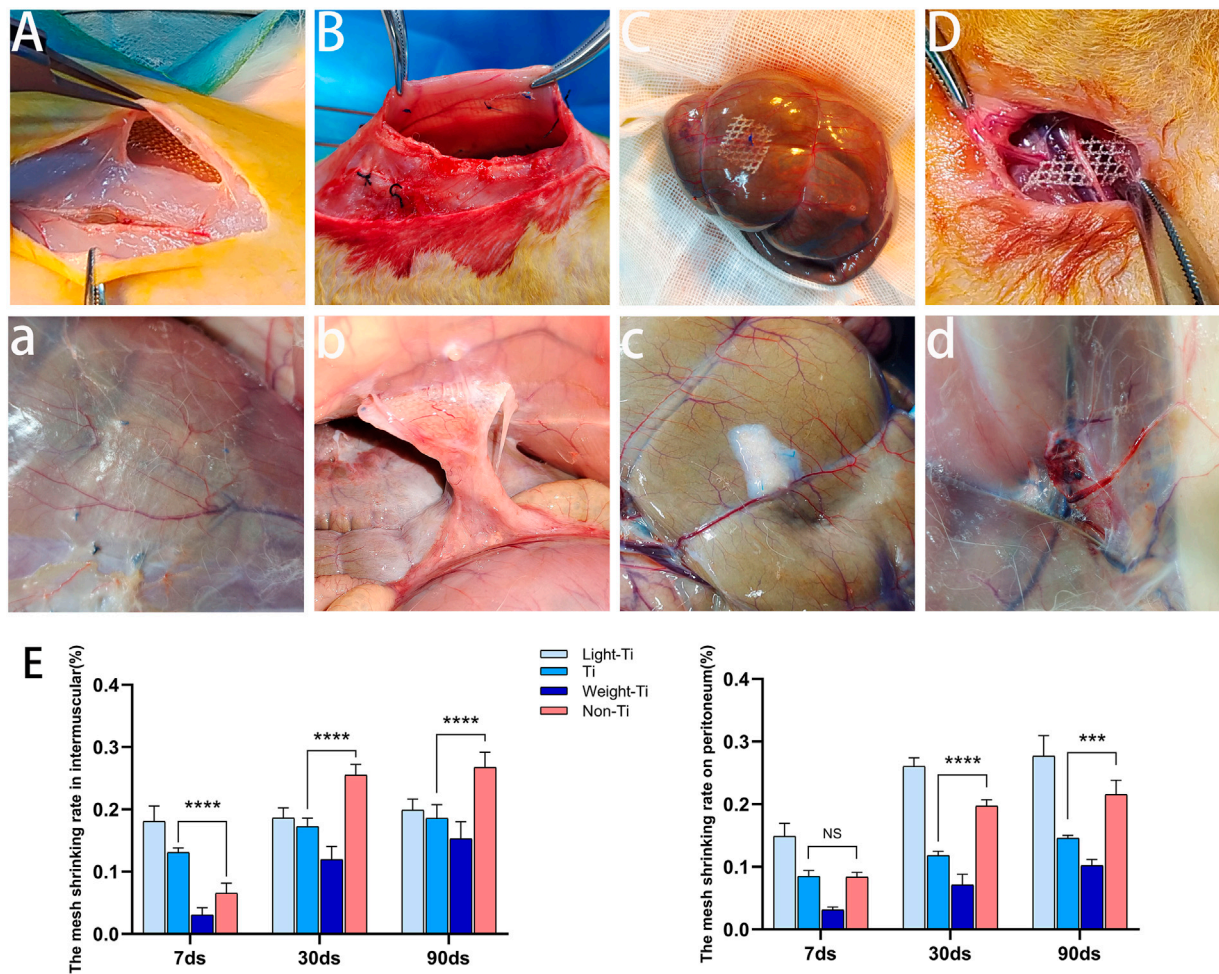
FIGURE 3
The conditions of meshes during operation and dissection and the shrinkage rate of meshes. **(A)** The mesh placed between the external oblique abdominal muscle and the internal oblique abdominal muscle during operation; **(A)** The mesh placed between the abdominal muscles at dissection; **(B)** The mesh placed on the parietal peritoneum during operation; **(B)** The mesh placed on the parietal peritoneum at dissection; **(C)** The mesh placed on the wall of the descending colon during operation; **(C)** The mesh placed on the wall of the descending colon at dissection; **(D)** The mesh placed under the femoral nerve during operation; **(D)** The mesh placed under the femoral nerve at dissection; **(E)** the shrinkage rate of meshes placed between the external oblique abdominal muscle and the internal oblique abdominal muscle and on the parietal peritoneum.

mode. In Group p, the Light-Ti group had the largest number of folds (6/24), followed by Non-Ti group (5/24).

3.4 Mesh adhesions

The SMSG score was used to score the adhesion of Group P. At three observation time points, the total adhesion score of the Non-Ti group was higher than that of the Ti group, but there was no statistical relationship between the different groups. The adhesion degree of all groups was the most serious at 30 days after the operation. After entering the chronic inflammatory period (90 days), the adhesion in each group improved, and the Ti group and Weight-Ti group demonstrated the most significant improvement. (The data are in Supplementary Table S2).

3.5 Mesh shrinkage

In the acute inflammatory period (7 days), the shrinkage rate of the Non-Ti group was slightly lower than that of the Ti group in Group M, but after the subacute period (30 days), the shrinkage rate of the Non-Ti group continued to increase and far exceeded that of the other three groups. After the chronic inflammatory period (90 days), the shrinkage rate of the four groups showed no significant changes. Regardless of the period, the shrinkage rate of the titanized polypropylene mesh in the intermuscle region decreased with their type. Comparing shrinkage rates in the acute inflammatory period with the chronic inflammatory period, the largest change in shrinkage rate was observed in the Non-Ti group.

The results of Group p revealed that there was no significant difference in the shrinkage rate between the Ti group and the Non-Ti group in the acute inflammatory period, but after entering the
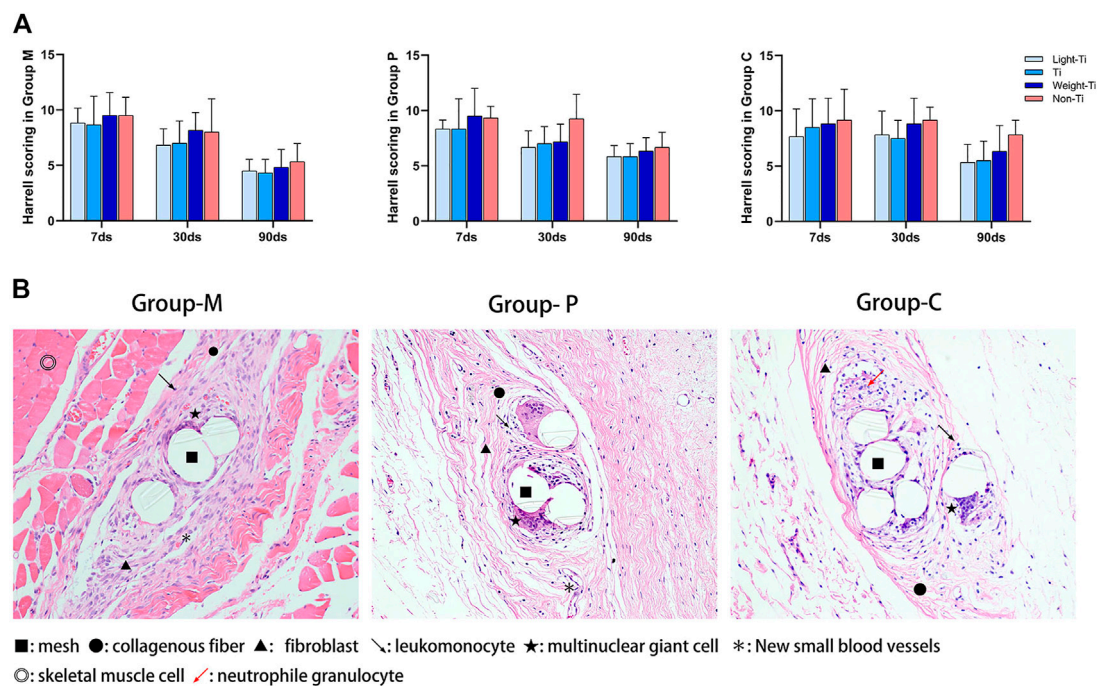
FIGURE 4
HE staining and its Harrell Scoring scale results. **(A)** Harrell Scoring scale results of different parts were obtained according to HE staining; **(B)** The situation of the mesh and the surrounding tissue between the external oblique abdominal muscle and the internal oblique abdominal muscle, on the parietal peritoneum, and on the wall of the descending colon. (HE staining, ×100 magnification).

subacute inflammatory period, the shrinkage rate of the Non-Ti group was higher than that of the Ti group and gradually increased. Although the shrinkage rate of the Light-Ti mesh on the parietal peritoneum gradually decreased with the increase in mesh type, the shrinkage rate of the Light-Ti group was still much higher than that of the other three meshes. Not only that, the probability of folding after operation in the Light-Ti group was the largest (6/24) (Shown in Figure 3E).

3.6 Inflammation

Hematoxylin-eosin staining was performed on the mesh and its surrounding tissue to evaluate the condition of granulation connective tissue and the level of inflammatory response around the mesh at different periods and different locations. The data showed that the level of inflammation around the mesh decreased with time in Group M, Group p and Group C, but the level of inflammation in the Non-Ti group was higher than that of the Ti group, regardless of period or location. Moreover, the difference between the three titanized polypropylene meshes was not very obvious. Figure 4.

3.7 Fibrosis

3.7.1 Sirius red staining

Under a polarized light microscope, in Group M and Group p, it was found that there was more type I collagen in group Ti during the acute inflammatory period. After the chronic inflammatory period,

there was more type I collagen in the Non-Ti group, and the surrounding granuloma tissue was more mature. However, in Group C, the ratio of type I to type III collagen in the Non-Ti group was higher than that in the Ti group at all observation points. In addition, it was noted that the ratio of type I to type III collagen decreased gradually with the increase of titanium loading of titanized polypropylene meshes in Group M, Group p, and Group C (Shown in Figure 5).

3.7.2 Intercellular adhesion molecules

The expression of ICAM-1 and FN in the tissue around the mesh showed a similar trend in Group M, Group p, and Group C. At each observation time point, the expression of ICAM-1 and FN in the Non-Ti group was higher than the Ti group, thus indicating a higher degree of fibrosis in the Non-Ti group. The degree of fibrosis decreased with the titanized polypropylene mesh type.

3.8 Nerve damage and regeneration

The immunohistochemistry results of nerve tissue in the chronic inflammation period were compared. The expression of Caspase-3 in the Non-Ti group was the highest and significantly higher than that in the Ti group ($p < 0.0001$), but no significant difference was found in the three titanized polypropylene meshes. Between the Non-Ti and Ti groups, there was no significant difference in the expression of MAP-2, which indicated nerve regeneration, but the Light-Ti group appeared to be better than the Non-Ti group in promoting nerve tissue regeneration ($p = 0.009$). In addition, the expression of GAP43, another nerve regeneration marker, was
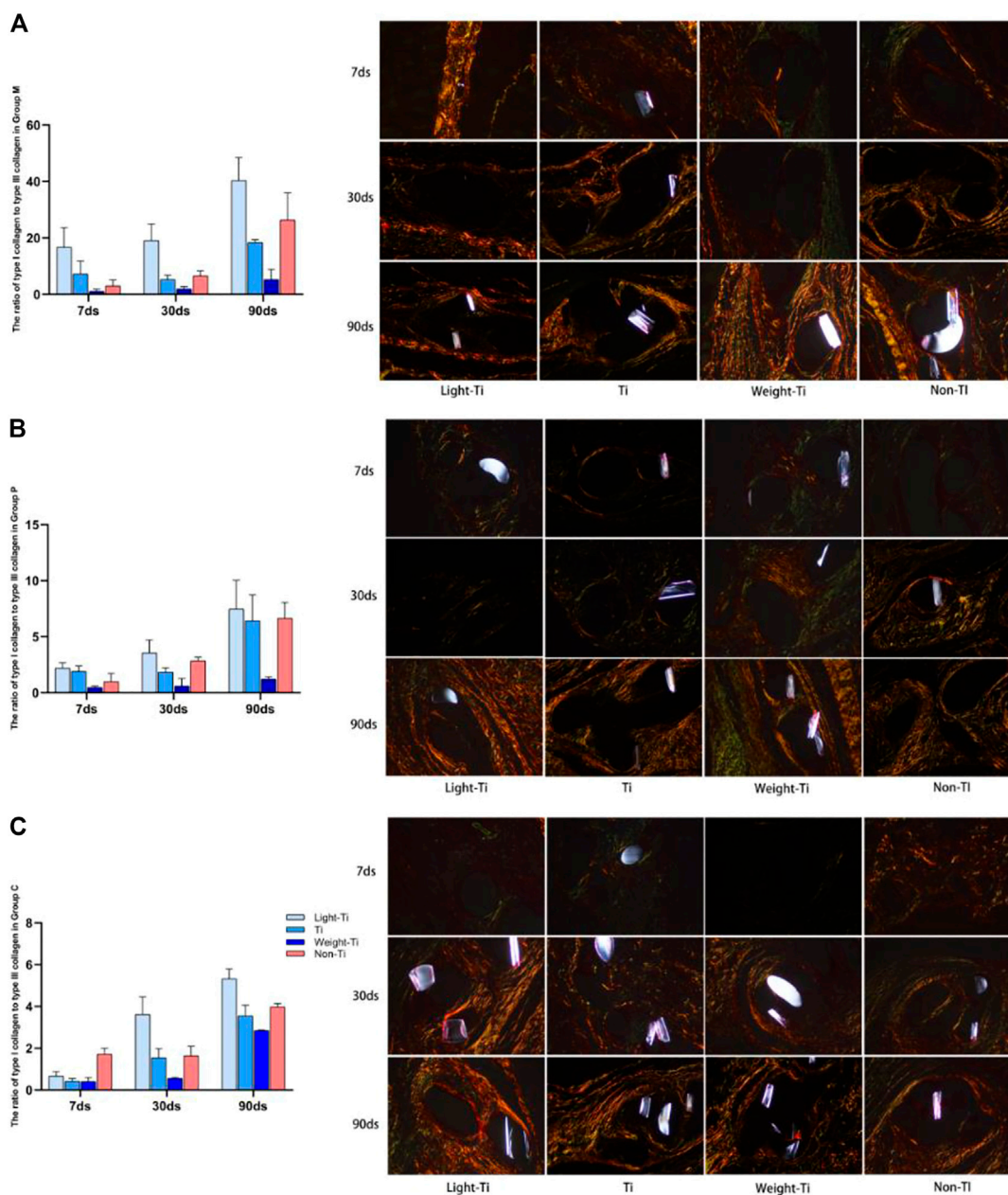
FIGURE 5
Sirius red staining and its ratio of type I to type III collagen. **(A)**: meshes between the external oblique abdominal muscle and the internal oblique abdominal muscle; **(B)**: meshes on the parietal peritoneum; **(C)**: meshes on the wall of the descending colon. (Sirius red staining, ×200 magnification).

significantly higher in the Ti group than in the Non-Ti group ($p <$ 0.0001), Furthermore, the Light-Ti group was also more conducive to nerve tissue regeneration than the Weight-Ti group (Figures 6C, D).

4 Discussion

Although the clinical use of mesh in abdominal external hernia repair effectively reduces the postoperative recurrence rate, it also causes mesh-related complications. For this reason, researchers

continue to search for the "perfect" mesh material, one which can not only meet the clinical requirements but also minimize complications. In a titanized polypropylene mesh, a titanium compound is added to the surface of the polypropylene filament based on various physical and chemical principles. It endows the polypropylene material with the excellent physical and chemical properties of the titanium element. The resulting better biocompatibility could reduce the adverse complications caused by polypropylene meshes, such as organ erosion. To sum up the previous *in vitro* cell experiments related to titanium-polypropylene mesh and abdominal external hernia, most experiments explored

FIGURE 6
Immunohistochemistry of the tissues. **(A)** ICAM-1 expression in tissues of each group; **(B)** FN expression in tissues of each group; **(C)** immunohistochemical staining of nerve tissues in Ti group and Non-Ti group at ×90days (immunohistochemical staining, ×400 magnification); **(D)** expression of Caspase-3, Map-2 and GAP-43 in each mesh groups at 90 days.
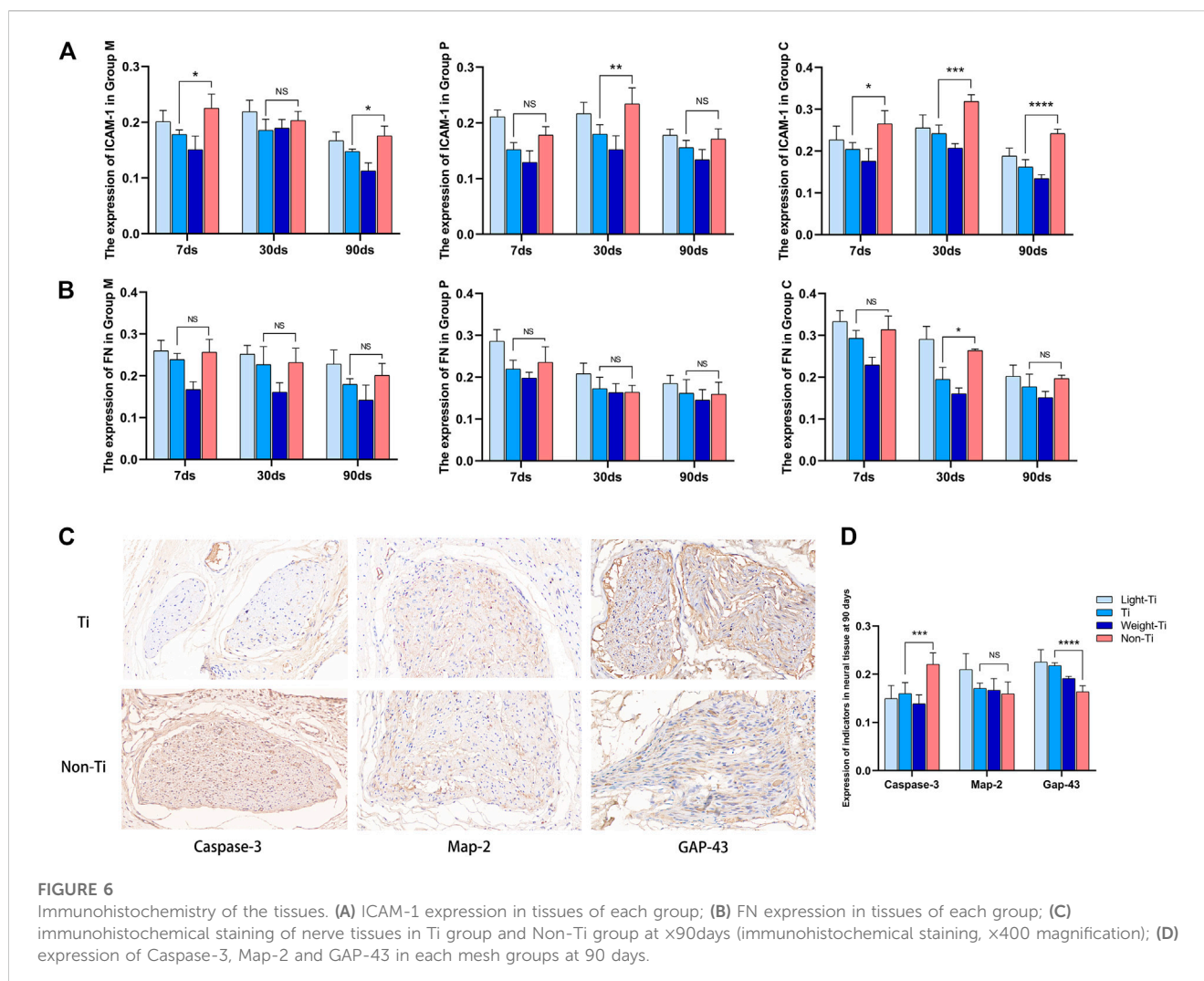
the antibacterial properties or fixation effects (i.e., mechanics) of different meshes, and none of them could conclude that the titanium polypropylene mesh has obvious advantages (Schug-Pass et al., 2009; Schug-Pass et al., 2010; Schug-Pass et al., 2012a; Schug-Pass et al., 2012b; Sanders et al., 2013). In an experimental study that simulated the cellular environment of breast reconstruction, titanized polypropylene meshes were compared with a partially absorbable mesh and a biological mesh. In terms of cytotoxicity, cell proliferation, and oxidative stress, the titanized polypropylene meshes did not seem to possess any obvious advantages (Dieterich et al., 2014). However, another cell test in which titanized polypropylene meshes were co-cultured with three biological mesh and immune cells showed that titanized polypropylene meshes exerted less stimulation on cells and reduced the level of immune inflammatory response. The authors believed this to be the reason why titanized polypropylene meshes caused less red chest syndrome in breast reconstruction (Karsten et al., 2018). So far, we have not found any cell experiments *in vitro* that simulate the environment of abdominal external hernias. Therefore, in order to confirm the role of titanium compound in the modification of polypropylene material, we simulated the cellular environment of abdominal external hernia repair and compared the titanium-loaded

polypropylene material with pure polypropylene material, that had almost the same physical parameters.

In order to simulate the important structures in the abdominal external hernia environment, HSF were used to represent the subcutaneous connective tissue, HMrSV5 were used to represent the parietal peritoneum, the inflammatory environment was represented by activated THP-1, and they were co-cultured with the two meshes. The cell proliferation assay indicated that cell proliferation was inhibited by the meshes, but the cells grown in the titanized polypropylene meshes environment seemed to be more inhibited, which we attributed to the effects of the titanium compound. In the apoptosis assay, it was observed that the existence of mesh could aggravate the apoptosis of cells, but the quantitative analysis showed that the titanium compound reduced the degree of apoptosis. Based on the results of the two groups of cell experiments, although the polypropylene meshes had a lower inhibition on cell proliferation, it also increased the degree of apoptosis at the same time. Therefore, in order to explore the dynamic results caused by the two factors, scanning electron microscope and confocal microscope experiments were conducted, and the growth of three kinds of cells on the mesh was directly observed. Finally, the number of cells adhering to the

surface of titanized polypropylene meshes was found to be significantly superior to that of the polypropylene mesh. This advantage is related to the content of the compound: increasing the amount of titanium compounds increases the attachment of cells to its surface. We believe that the titanized polypropylene mesh not only reduces the influence of the mesh on cell growth, but also promotes the "fixation" of cells on its surface by virtue of the "inertness", "hydrophilicity" and "cytophilicity" of its titanium coating. Therefore, the addition of titanium compounds did optimize the biocompatibility of polypropylene materials.

Previous animal experiments mostly compared the anti-adhesion and anti-shrinkage properties of titanized polypropylene meshes with other types of meshes. Compared with various inorganic meshes, partially absorbable meshes, and biological meshes, titanized polypropylene meshes have been found to have uneven performance. In some experiments, the adhesion degree of the titanized polypropylene mesh was noted to be similar to that of other reticulated mesh, while no-reticulated mesh or biological mesh showed significant anti-adhesion advantages. However, some studies directly confirmed the anti-adhesion function of titanized polypropylene mesh, and researchers think that the low shrinkage rate of titanized polypropylene mesh was also related to its low adhesion rate and low inflammatory response (Schug-Pass et al., 2006; Schug-Pass et al., 2008; Delibegovic et al., 2016; Bouliaris et al., 2019). After summarizing the results of these studies, we found that the variables (raw material, preparation structure, weight, etc.) among various meshes were not singular, and direct comparison could not adequately summarize the influencing factors.

Furthermore, in many experiments, pure polypropylene meshes used for comparison with titanized polypropylene meshes were all of medium weight, such as Prolene® and Atrium® (Scheidbach et al., 2003; Burger et al., 2006; Schreinemacher et al., 2009; Bouliaris et al., 2019). In fact, these are unable to control variables sufficiently enough to explore whether titanium compounds improve the performance of polypropylene materials. Therefore, after taking note of these variables, we selected a titanized polypropylene mesh (PFM, Germany) with very similar physical parameters to compare with a pure polypropylene mesh (B.Braun, Spain). In addition, different types of titanized polypropylene meshes were used as a supplement for *in vivo* animal experiments.

In animal experiments performed in our study, it was found that in different periods, the anti-adhesion of the polypropylene mesh seemed to be inferior to that of the light titanized polypropylene mesh, Furthermore, in terms of anti-shrinkage, only a certain degree of advantage was seen in the acute inflammatory stage (7days). Once the subacute inflammatory period (30days) was entered, its shrinkage rate was significantly higher than that of titanized polypropylene meshes. From our findings, whether it is anti-adhesion or anti-contraction performance, the addition of the titanium compound did produce a positive result. This effect seems to have a certain trend in different types of titanium polypropylene mesh: whether it is placed in the intermuscular or abdominal wall, the shrinkage rate of the mesh decreases with the type of titanium polypropylene mesh. Comparing these three types of mesh, we believe that this could be the result of the weaving process of the mesh, the amount of titanium loaded and other factors. However, it has to be mentioned that the anti-contraction performance of the Light-Ti group in Group *p* is not excellent, and even after entering the chronic inflammatory period,

the contraction rate is still greater than that of the Non-Ti group. At the same time, during the placement process, we could feel that the meshes in the Light-Ti group were too soft, and the probability of folding was the highest during the dissection, which may be one of the reasons why it is rarely used in clinical treatment. The paraffin-fixed specimens were then stained with sirius red. The ratio of type I collagen to type III collagen in the granulation tissue around the mesh was higher in Group M, Group *p*, and Group C under a polarized light microscope, indicating that the granulation tissue around the mesh was more mature. A previous clinical study found that more than 70% of specimens removed from patients after recurrent hernia repair showed a reduced ratio of type I to type III collagen, and the ratio and degree of intermolecular cross-linking of type I and type III collagen affect the tensile strength and mechanical stability of connective and scar tissue. However, this observation supports the hypothesis that the alteration of the extracellular matrix is the main pathophysiological cause of hernia recurrence; it is not the mesh shrinkage, but the simple contraction of fibrotic scar tissue surrounding the mesh that leads to the reduction of mesh area (Klosterhalfen et al., 2004; Klosterhalfen et al., 2005). Taking that into account in our experiments, the rate of shrinkage of the mesh between the intermuscular and abdominal wall was surprisingly consistent with the ratio trend of type I and type III collagen in the tissues around the mesh. With ICAM-1 and FN analyses, which evaluate the degree of fibrosis, the trend was generally consistent with the results of the first two experiments. Therefore, our experimental results also support the hypothesis that changes in the extracellular matrix lead to reduction of in mesh area. At the same time, we identified similar results in many foreign animal experiments using HE staining: the level of inflammatory reaction in different parts of the titanized polypropylene mesh was lower than that of the polypropylene mesh. Whether this result is truly related to the lower shrinkage of the titanized polypropylene mesh needs to be further verified in follow-up experiments.

Finally, we took the lead in carrying out a preliminary experiment on the neural damage caused by the mesh. Immunohistochemical analysis of the nerve tissue around the mesh showed that MAP-2 and GAP-43, which play a highly positive role in nerve regeneration, were less expressed in the polypropylene mesh. Moreover, the obvious increase of Caspase-3 suggests that the polypropylene mesh exerts more damage on nerve tissue. We believe that this may be related to reduced chronic pain after inguinal hernia surgery with the titanized polypropylene mesh. Our experimental results show that the titanium compounds has fewer effects on the nerve tissue, and it is, therefore, more conducive to the regeneration of nerve fibers.

5 Conclusion

Titanium compounds can improve the biocompatibility of polypropylene materials, reduce the influence of polypropylene materials on cell growth, and facilitate cell fixation and adhesion. At the same time, the titanized polypropylene mesh has better effects in terms of anti-adhesion, anti-contraction and the degree of tissue fibrosis. Furthermore, it can also reduce damage to the nerve, but such performance depends on the type of mesh and the placement environment.

The above conclusions are based on this cell and animal experiment, but this is not sufficient to prove that these conclusions are clinically relevant. At present, due to ethics and other factors, we are temporarily unable to obtain human tissue specimens for further experiment. However, we hope to see research data based on human tissue published in the future.

Data availability statement

The original contribution presented in the study are included in the article/Supplementary Material, further inquiries can be directed to the corresponding author.

Ethics statement

The animal experimental protocol was approved by the Medical Research Ethics Committee of Chongqing Medical University (approval number: 2022-K302, date: 20 June 2022). All experiments were performed in accordance with the Laboratory Animal Care and Use Guide issued by the Ministry of Science and Technology.

Author contributions

Contributions: Conception and design: YX and YZ; Administrative support: YZ and XW; Provision of study materials or patients: XY and XW; Collection and assembly of data: XY and XH; Data analysis and interpretation: XY, XH and GY; Manuscript writing: YX; Final approval of manuscript: All authors.

Conflict of interest

The authors declare that the research was conducted in the absence of any commercial or financial relationships that could be construed as a potential conflict of interest.

Publisher's note

All claims expressed in this article are solely those of the authors and do not necessarily represent those of their affiliated organizations, or those of the publisher, the editors and the reviewers. Any product that may be evaluated in this article, or claim that may be made by its manufacturer, is not guaranteed or endorsed by the publisher.

Supplementary material

The Supplementary Material for this article can be found online at: https://www.frontiersin.org/articles/10.3389/fmats.2023.1125766/full#supplementary-material

References

Aydemir Sezer, U., Sanko, V., Gulmez, M., Aru, B., Sayman, E., Aktekin, A., et al. (2019). Polypropylene composite hernia mesh with anti-adhesion layer composed of polycaprolactone and oxidized regenerated cellulose. *Mater Sci. Eng. C Mater Biol. Appl.* 99, 1141–1152. doi:10.1016/j.msec.2019.02.064

Aydemir Sezer, U., Sanko, V., Gulmez, M., Sayman, E., Aru, B., Yuksekdag, Z. N., et al. (2017). A polypropylene-integrated bilayer composite mesh with bactericidal and antiadhesive efficiency for hernia operations. *ACS Biomater. Sci. Eng.* 3 (12), 3662–3674. doi:10.1021/acsbiomaterials.7b00757

Baylon, K., Rodriguez-Camarillo, P., Elias-Zuniga, A., Diaz-Elizondo, J., Gilkerson, R., and Lozano, K. (2017). Past, present and future of surgical meshes: A review. *Membr. (Basel)* 7 (3), 47. doi:10.3390/membranes7030047

Bland, K. I. (2008). Randomized clinical trial of Lichtenstein's operation versus mesh plug for inguinal hernia repair. *Yearb. Surg.* 2008, 320–321. doi:10.1016/s0090-3671(08)79217-6

Bouliaris, K., Asprodini, E., Liakos, P., Diamantis, A., Koukoulis, G., Befani, C., et al. (2019). Adhesion prevention to polypropylene meshes using combined icodextrin four percent and dimetindene maleate. *J. Surg. Res.* 234, 325–333. doi:10.1016/j.jss.2018.10.003

Burger, J. W., Halm, J. A., Wijsmuller, A. R., Raa, S., and Jeekel, J. (2006). Evaluation of new prosthetic meshes for ventral hernia repair. *Surg. Endosc.* 20 (8), 1320–1325. doi:10.1007/s00464-005-0706-4

Celik, A., Altinli, E., Koksal, N., Onur, E., and Ozkan, O. F. (2009). The shrinking rates of different meshes placed intraperitoneally A long-term comparison of the TiMesh, vypro II, sepramesh, and DynaMesh. *Surg. Laparosc. Endosc. Percutan Tech.* 19 (4), e130–e134. doi:10.1097/sle.0b013e3181aa598d

Chamberlain, L. M., Godek, M. L., Gonzalez-Juarrero, M., and Grainger, D. W. (2009). Phenotypic non-equivalence of murine (monocyte-) macrophage cells in biomaterial and inflammatory models. *J. Biomed. Mater. Res. Part A* 88A (4), 858–871. doi:10.1002/jbm.a.31930

D'Amore, L., Ceci, F., Mattia, S., Fabbi, M., Negro, P., and Gossetti, F. (2017). Adhesion prevention in ventral hernia repair: An experimental study comparing three lightweight porous meshes recommended for intraperitoneal use. *Hernia* 21 (1), 115–123. doi:10.1007/s10029-016-1541-3

Daigneault, M., Preston, J. A., Marriott, H. M., Whyte, M. K. B., and Dockrell, D. H. (2010). The identification of markers of macrophage differentiation in PMA-stimulated THP-1 cells and monocyte-derived macrophages. *PLoS One* 5 (1), e8668. doi:10.1371/journal.pone.0008668

Delibegovic, S., Koluh, A., Cickusic, E., Katica, M., Mustedanagic, J., and Krupic, F. (2016). formation of adhesion after intraperitoneal application of TiMesh: Experimental study on a rodent model. *Acta Chir. Belg* 116 (5), 293–300. doi:10.1080/00015458.2016.1179513

Dieterich, M., Stubert, J., Gerber, B., Reimer, T., and Richter, D. U. (2014). Biocompatibility, cell growth and clinical relevance of synthetic meshes and biological matrixes for internal support in implant-based breast reconstruction. *Arch. Gynecol. Obstet.* 291 (6), 1371–1379. doi:10.1007/s00404-014-3578-9

Elango, S., Perumalsamy, S., Ramachandran, K., and Vadodaria, K. (2017). Mesh materials and hernia repair. *Biomed. (Taipei)* 7 (3), 16. doi:10.1051/bmdcn/2017070316

Filipović-Čugura, J., Misir, Z., Hrabac, P., Oresic, T., Vidovic, D., Misir, B., et al. (2020). Comparison of surgisis, vypro II and TiMesh in contaminated and clean field. *Hernia* 24 (3), 551–558. doi:10.1007/s10029-019-01949-1

Frey, D. M., Wildisen, A., Hamel, C. T., Zuber, M., Oertli, D., and Metzger, J. (2007). Randomized clinical trial of Lichtenstein's operation versus mesh plug for inguinal hernia repair. *Br. J. Surg.* 94 (1), 36–41. doi:10.1002/bjs.5580

Gordon, S. (2007). The macrophage: Past, present and future. *Eur. J. Immunol.* 37 (1), S9–S17. doi:10.1002/eji.200737638

Halm, J. A., de Wall, L. L., Steyerberg, E. W., Jeekel, J., and Lange, J. F. (2007). Intraperitoneal polypropylene mesh hernia repair complicates subsequent abdominal surgery. *World J. Surg.* 31 (2), 423–429. discussion 430. doi:10.1007/s00268-006-0317-9

Harrell, A. G., Novitsky, Y. W., Cristiano, J. A., Gersin, K. S., Norton, H. J., Kercher, K. W., et al. (2007). Prospective histologic evaluation of intra-abdominal prosthetics four months after implantation in a rabbit model. *Surg. Endosc.* 21 (7), 1170–1174. doi:10.1007/s00464-006-9147-y

Hu, W., Zhang, Z., Lu, S., Zhang, T., Zhou, N., Ren, P., et al. (2018). Assembled anti-adhesion polypropylene mesh with self-fixable and degradable *in situ* mussel-inspired hydrogel coating for abdominal wall defect repair. *Biomaterials Sci.* 6 (11), 3030–3041. doi:10.1039/c8bm00824h

Junge, K., Rosch, R., Klinge, U., Saklak, M., Klosterhalfen, B., Peiper, C., et al. (2004). Titanium coating of a polypropylene mesh for hernia repair: Effect on biocompatibilty. *Hernia* 9 (2), 115–119. doi:10.1007/s10029-004-0292-8

Junqueir, L. C. U. (1978). Differential staining of collagens and polarization type I, II and III by sirius red microscopy. *Arch. Histol. Jpn.* 41 (3), 267–274.

Kajiyama, H., Shibata, K., Ino, K., Nawa, A., Mizutani, S., and Kikkawa, F. (2007). Possible involvement of SDF-1α/CXCR4-DPPIV axis in TGF-β1-induced enhancement of migratory potential in human peritoneal mesothelial cells. *Cell Tissue Res.* 330 (2), 221–229. doi:10.1007/s00441-007-0455-x

Karsten, M. M., Enders, S., Knabl, J., Kirn, V., Duwell, P., Rack, B., et al. (2018). Biologic meshes and synthetic meshes in cancer patients: A double-edged sword: Differences in production of IL-6 and IL-12 caused by acellular dermal matrices in human immune cells. *Arch. Gynecol. Obstet.* 297 (5), 1265–1270. doi:10.1007/s00404-018-4710-z

Klosterhalfen, B., Junge, K., and Klinge, U. (2005). The lightweight and large porous mesh concept for hernia repair. *Expert Rev. Med. Devices* 2 (1), 103–117. doi:10.1586/17434440.2.1.103

Klosterhalfen, B., Klinge, U., Rosch, R., and Junge, K. (2004). *Long-term inertness of meshes.* Heidelberg, Germany: Springer Berlin Heidelberg.

Leber, G. E., Garb, J. L., Alexander, A. I., and Reed, W. P. (1998). Long-term complications associated with prosthetic repair of incisional hernias. *Arch. Surg.* 133 (4), 378–382. doi:10.1001/archsurg.133.4.378

Listed, N. (1992). Prophylaxis of pelvic sidewall adhesions with gore-tex surgical membrane: A multicenter clinical investigation. The surgical membrane study group. *Fertil. Steril.* 57 (4), 921–923.

Mosser, D. M., and Edwards, J. P. (2008). Exploring the full spectrum of macrophage activation. *Nat. Rev. Immunol.* 8 (12), 958–969. doi:10.1038/nri2448

Pereira-Lucena, C. G., Artigiani-Neto, R., Lopes-Filho, G. J., Frazao, C. V. G., Goldenberg, A., Matos, D., et al. (2010). Experimental study comparing meshes made of polypropylene, polypropylene + polyglactin and polypropylene + titanium: Inflammatory cytokines, histological changes and morphometric analysis of collagen. *Hernia* 14 (3), 299–304. doi:10.1007/s10029-009-0621-z

Ross, S. W., and Iannitti, D. A. (2019). "Chapter 55 - mesh: Material science of hernia repair," in *Shackelford's surgery of the alimentary tract, 2 volume set.* Editor C. J Yeo. Eighth Edition (Philadelphia: Elsevier), 621–632.

Russo Serafini, M., Medeiros Savi, F., Ren, J., Bas, O., O'Rourke, N., Maher, C., et al. (2021). The patenting and technological trends in hernia mesh implants. *Tissue Eng. Part B Rev.* 27 (1), 48–73. doi:10.1089/ten.teb.2019.0245

Sanders, D., Lambie, J., Bond, P., Moate, R., and Steer, J. A. (2013). An *in vitro* study assessing the effect of mesh morphology and suture fixation on bacterial adherence. *Hernia* 17 (6), 779–789. doi:10.1007/s10029-013-1124-5

Scheidbach, H., Tamme, C., Tannapfel, A., Lippert, H., and Köckerling, F. (2003). *In vivo* studies comparing the biocompatibility of various polypropylene meshes and their handling properties during endoscopic total extraperitoneal (TEP) patchplasty: An experimental study in pigs. *Surg. Endosc.* 18 (2), 211–220. doi:10.1007/s00464-003-8113-1

Schopf, S., von Ahnen, T., von Ahnen, M., and Schardey, H. (2011). Chronic pain after laparoscopic transabdominal preperitoneal hernia repair: A randomized comparison of light and extralight titanized polypropylene mesh. *World J. Surg.* 35 (2), 302–310. doi:10.1007/s00268-010-0850-4

Schreinemacher, M. H., Emans, P. J., Gijbels, M. J. J., Greve, J. W. M., Beets, G. L., and Bouvy, N. D. (2009). Degradation of mesh coatings and intraperitoneal adhesion formation in an experimental model. *Br. J. Surg.* 96 (3), 305–313. doi:10.1002/bjs.6446

Schug-Pass, C., Jacob, D. A., Lippert, H., and Kockerling, F. (2012). Differences in biomechanical stability using various fibrin glue compositions for mesh fixation in endoscopic inguinal hernia repair. *Surg. Endosc.* 26 (11), 3282–3286. doi:10.1007/s00464-012-2339-8

Schug-Pass, C., Jacob, D. A., Rittinghausen, J., Lippert, H., and Kockerling, F. (2012). Biomechanical properties of (semi-) synthetic glues for mesh fixation in endoscopic inguinal hernia repair. *Hernia* 17 (6), 773–777. doi:10.1007/s10029-012-1000-8

Schug-Pass, C., Lippert, H., and Köckerling, F. (2009). Fixation of mesh to the peritoneum using a fibrin glue: Investigations with a biomechanical model and an experimental laparoscopic porcine model. *Surg. Endosc.* 23 (12), 2809–2815. doi:10.1007/s00464-009-0509-0

Schug-Pass, C., Lippert, H., and Köckerling, F. (2010). Mesh fixation with fibrin glue (Tissucol/Tisseel) in hernia repair dependent on the mesh structure-is there an optimum fibrin-mesh combination?-investigations on a biomechanical model. *Langenbecks Arch. Surg.* 395 (5), 569–574. doi:10.1007/s00423-009-0466-z

Schug-Pass, C., Sommerer, F., Tannapfel, A., Lippert, H., and Kockerling, F. (2008). Does the additional application of a polylactide film (SurgiWrap) to a lightweight mesh (TiMesh) reduce adhesions after laparoscopic intraperitoneal implantation procedures? Experimental results obtained with the laparoscopic porcine model. *Surg. Endosc.* 22 (11), 2433–2439. doi:10.1007/s00464-008-9876-1

Schug-Pass, C., Tamme, C., Tannapfel, A., and Kockerling, F. (2006). A lightweight polypropylene mesh (TiMesh) for laparoscopic intraperitoneal repair of abdominal wall hernias. *Surg. Endosc.* 20 (3), 402–409. doi:10.1007/s00464-004-8277-3

Shin, H. S., Ryu, E. S., Oh, E. S., and Kang, D. H. (2015). Endoplasmic reticulum stress as a novel target to ameliorate epithelial-to-mesenchymal transition and apoptosis of human peritoneal mesothelial cells. *Lab. Invest.* 95 (10), 1157–1173. doi:10.1038/labinvest.2015.91

Wu, H., Li, Z., Tang, J., Yang, X., Zhou, Y., Guo, B., et al. (2019). The *in vitro* and *in vivo* anti-melanoma effects of hydroxyapatite nanoparticles: Influences of material factors. *Int. J. Nanomedicine* 14, 1177–1191. doi:10.2147/ijn.s184792